Philosophical Magazine Letters,
Vol. 85, No. 7, July 2005, 331–337

Thermal effects on pressure-induced infiltration of a nanoporous system

X. KONG and Y. QIAO*

Department of Civil Engineering, University of Akron,
Akron, OH 44325-3905, USA

(*Received 1 October 2004; in final form 12 February 2005*)

Thermal effects on the energy absorption efficiency of a system consisting of hydrophobic mesoporous silica particles immersed in water have been investigated. As the temperature increases, although the infiltration pressure decreases only slightly and the accessible pore volume remains nearly constant, the system recoverability can be significantly improved, primarily due to an increase in outflow pressure. The sequence of changing pressure and temperature has little influence on the system performance.

1. Introduction

Developing advanced energy absorption systems (EAS) is of immense importance to a variety of industrial areas such as construction, automobile, and defence. Usually, an EAS is based on materials that can dissipate a certain amount of energy by multiple-site failure or dispersed phase transformation [1]. Currently, the commonly used EAS materials include composites, shape-memory alloys, and foams, among others. While these materials have been of unquestionable utility, their energy absorption effectiveness is sometimes not able to satisfy the functional requirements. As a result, the protection system is often over-sized and/or over-weight. Over the years, new mechanisms have been explored to develop high-performance EAS, among which the use of nanoporous materials is a novel and promising technique [2–5].

When nanoporous particles are immersed in a non-wetting liquid, under atmosphere pressure, p_{at}, infiltration cannot occur spontaneously owing to the capillary effect. As the pressure increases, however, the liquid can be forced into the nanopores, accompanied by a significant increase in interfacial energy [6–8]. When the pressure is reduced to p_{at}, for reasons that are still quite inadequately understood, the outflow can be difficult, especially in mesoporous materials such as porous silicas [9]. Owing to the ultrahigh specific surface area, the specific absorbed energy can be much higher than that of conventional EAS materials.

*Corresponding author. Email: yqiao@uakron.edu

Philosophical Magazine Letters
ISSN 0950–0839 print/ISSN 1362–3036 online © 2005 Taylor & Francis
http://www.tandf.co.uk/journals
DOI: 10.1080/09500830500071135

While the hysteretic absorption behaviours of nanoporous materials have been noticed in the fields of chemical engineering and biosciences, the study on applying this phenomenon in protection devices is still at its early stage. The previous researches have been mostly proof-of-concept experiments. Test data involving a number of important factors, e.g. thermal effects, the influences of pore shapes, and pore/particle size distributions, are scarce. In this article, we report an experimental investigation on the behaviour of a nanoporous silica system at different temperatures. The results show that, as the temperature increases from 20°C to 80°C, there is a significant increase in system recoverability, while the variation in infiltration pressure is only secondary.

2. Experimental

The energy absorption system studied in the current research was based on Fluka 100 C_8 reversed-phase mesoporous silica. According to the gas absorption measurement performed at Quantachrome Instruments, the specific area is 287 m^2/g. The average pore size is 7.8 nm, with a standard deviation of 2.4 nm. The material is in powder form, and the particle size is in the range of 15–35 μm. The surface coverage, which is defined as the percentage of the surface area covered by functional groups, is 10–12%, leading to a high degree of hydrophobicity. Such nanoporous materials have been widely applied in chromatography.

The testing sample consisted of 0.5 g of the mesoporous silica particles immersed in deionized water, which was sealed in a compressible container. The details of the experimental device are documented elsewhere [9]. In a type 5569 Instron machine under displacement control mode, the system was compressed at a constant rate of 1 mm/min, and the pressure, p, increased continuously. Initially, under atmospheric pressure the water could not enter the nanopores. When the pressure reached about 17 MPa, infiltration started to occur in the relatively large pores, leading to an abrupt decrease in the slope of absorption isotherm, as shown in figure 1a.

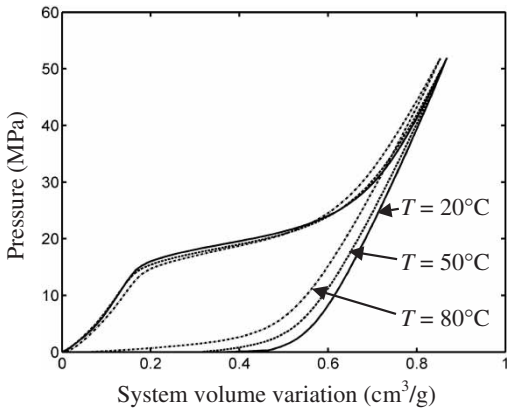

(a)

Figure 1. Sorption isotherms at different temperatures: (a) the first infiltration cycle; (b) the second infiltration cycle.

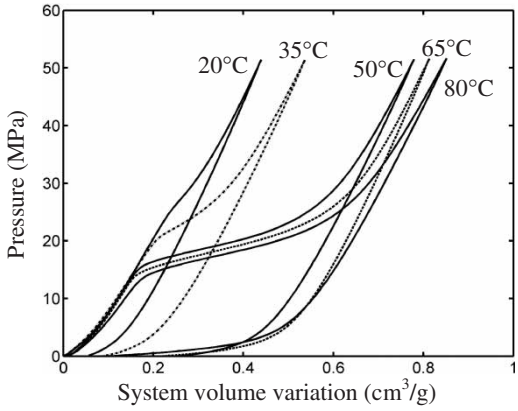

(b)

Figure 1. Continued.

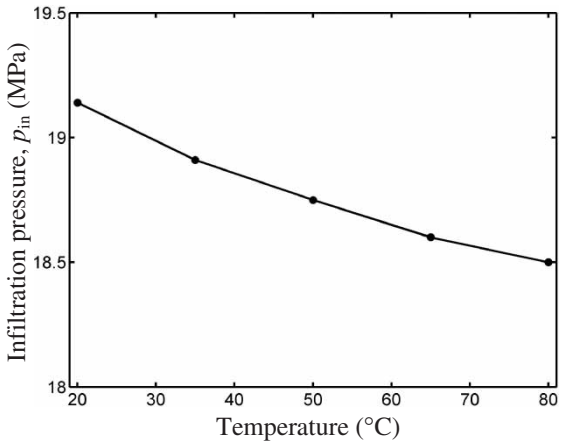

Figure 2. Thermal effect on the infiltration pressure.

As p exceeded about 24 MPa, most of the porous space was filled, and the slope of sorption isotherm increased rapidly. The effective infiltration pressure, p_{in}, was taken as the pressure at the middle point of the plateau region. When the pressure exceeded about 50 MPa, the applied load was reduced back to 0. The loading–unloading cycle was repeated for four times.

The infiltration tests were performed at different temperatures. The sorption isotherm curves for the first two infiltration cycles are shown in figure 1. The thermal effect on p_{in} is shown in figure 2. Figure 3 shows the temperature dependence of energy absorption effectiveness, E^*, which is calculated as the area enclosed by the hysteresis loop of sorption isotherm. Note that E^* indicates the energy absorbed by 1 g of nanoporous silica particles. The outflow pressure, which is defined as the pressure at the point in the unloading section of the first infiltration cycle where the slope of the sorption isotherm is reduced by 50%, is shown in table 1 as a function of temperature.

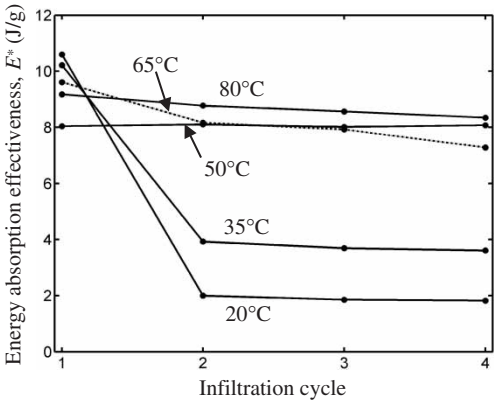

Figure 3. System recoverability at different temperatures.

Table 1. The outflow pressure as a function of temperature.

Temperature (°C)	20	35	50	65	80
Outflow pressure (MPa)	2.2	2.6	3.4	3.9	5.1

3. Results and discussion

According to figure 1a, for the first loading–unloading cycle, the widths of the plateau regions at different temperatures are about the same, indicating that the accessible specific volume is not sensitive to the temperature, T. However, the infiltration pressure, p_{in}, decreases consistently with temperature (see figure 2). When T rises from 20°C to 80°C, p_{in} is lowered by about 0.7 MPa. Based on classic surface theory, as a first-order approximation, the infiltration pressure required to overcome the capillary effect can be estimated as [10]

$$p_{in} = \frac{2\Delta\gamma}{r} \tag{1}$$

where r is the pore radius and $\Delta\gamma = \gamma_{SL} - \gamma_{SG}$ is the difference between the solid–liquid interfacial energy, γ_{SL}, and the surface energy of the solid, γ_{SG}. Note that since the nanoporous particles are hydrophobic, $\Delta\gamma > 0$. Both γ_{SG} and γ_{SL} are dependent of temperature. The $\gamma_{SG} - T$ relation can be described by a power-law function [11]

$$\gamma_{SG} = C_1 G_m + C_2 (T_m - T)^m \tag{2}$$

where C_1 and C_2 are material constants in the ranges of 0.5–3 and 0.2–0.6, respectively; G_m is the free energy of melting; T_m is the melting point; and m is a material constant in the range of 1–1.2. Usually, especially when the temperature range under consideration is much lower than T_m, a linear simplification can be used [12, 13]

$$\gamma_{SG} = \gamma_0 - \alpha T \tag{3}$$

where γ_0 is the reference surface energy and α is the temperature sensitivity.

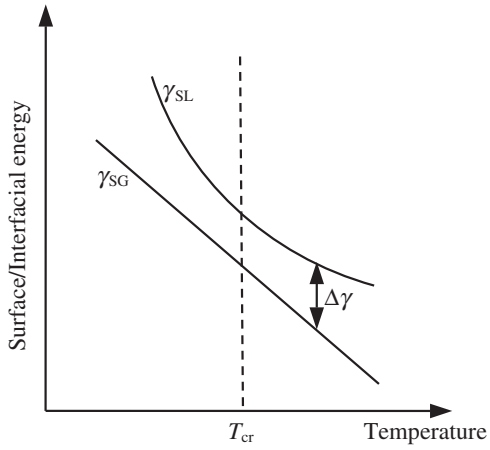

Figure 4. Schematic diagram of the temperature dependence of $\Delta\gamma$.

The $\gamma_{SL} - T$ relation, on the other hand, is usually highly nonlinear. Through the Clapeyron equation [14],

$$q_{st} = RT^2\left(\frac{\partial \ln p}{\partial T}\right)_{\Gamma} \tag{4}$$

where q_{st} is the isosteric heat, $\Gamma = H_p p$, $H_p = 1/k_B T\int_0^\infty[\exp(-\varphi(z)/k_B T) - 1]\,dz$ is the Henry constant, k_B is the Boltzmann constant, and $\varphi(z)$ is the potential energy along the normal of the interface, z. At zero loading we have [14]

$$\frac{q_{st}^{(0)}}{k_B T} = f\left(\frac{\gamma_{SL}}{k_B T}, \sigma_{sf}\right) \tag{5}$$

where σ_{sf} is the collision diameter and f is a nonlinear function determined by the $p - T$ relation. As depicted in figure 4, since $\partial\gamma_{SL}/\partial T$ and $\partial\gamma_{SG}/\partial T$ are different, there exists a critical temperature, T_{cr}, at which $\partial\gamma_{SL}/\partial T = \partial\gamma_{SG}/\partial T$. At T_{cr}, $\Delta\gamma$ is minimized. When $T < T_{cr}$, as temperature increases $\Delta\gamma$ decreases; and when $T > T_{cr}$, $\Delta\gamma$ increases with T. The experimental data of p_{in} indicate that in the temperature range under investigation, $\partial\Delta\gamma/\partial T < 0$, that is, T_{cr} is higher than 80°C. Note that, owing to the confinement effect of pore walls and the mass/energy exchange between gas/liquid phases, the interfacial energy in the nanoenvironment can be quite different from that in a macroscopic case.

For the second and the following infiltration cycles, the thermal effect is much more pronounced, as shown in figure 1b. At 20°C, the infiltration pressure associated with the second loop is much higher than that in the first loop. As T rises, p_{in} decreases rapidly and when $T > 50$°C, the difference of p_{in} in different loading–unloading cycles is negligible. A more significant effect is that the system recoverability increases considerably with temperature. When the temperature is relatively low, owing to the phenomenon of non-outflow, the porous space remains being occupied after unloading, and therefore the energy absorption effectiveness after the first infiltration cycle is nearly zero (see figure 3). When $T > 50$°C, E^* decreases only slightly after unloading, that is, under this condition the system is

nearly fully recoverable. If the infiltration tests are performed at room temperature, but in between the loading–unloading cycles the system is thermally treated at different temperatures, the sorption isotherm curves are about the same, i.e. the sequence of the thermal treatment and the infiltration test does not affect E^*. This phenomenon has great potential in reactivating nanoporous protection devices.

The thermal effect on E^* should be attributed to the temperature dependence of the outflow pressure, p_{out}. At relatively low temperatures, even under p_{at}, the confined liquid cannot come out of the nanopores. At an elevated temperature, especially when $T > 50^\circ$C, p_{out} is much higher and as a result most of the confined liquid can be released. As discussed above, the desorption process is insensitive to the pressure.

4. Conclusions

Thermal effects on the performance of an energy absorption system consisting of hydrophobic mesoporous silica particles have been investigated experimentally. Through the loading–unloading tests at different temperatures, the sorption isotherm curves are characterized by p_{in} and E^*. While the influence of temperature variation on p_{in} is only secondary, the outflow of the confined liquid is strongly dependent of thermal treatment, indicating that the mechanisms of the pressure induced absorption and desorption are different. The following conclusions are drawn:

(1) As temperature increases, the infiltration pressure decreases slightly.
(2) Temperature has little influence on the accessible specific pore volume.
(3) The efficiency of energy absorption associated with the first infiltration cycle is quite insensitive to the temperature.
(4) The system recoverability increases rapidly with temperature. When the temperature exceeds about 50°C, the system becomes almost fully reusable.
(5) The outflow is a thermally aided process and insensitive to pressure.

Acknowledgements

This study has been supported by the Army Research Office under Grant W911NF-04-1-0244, for which we are grateful to Dr David M. Stepp. Special thanks are also due to Dr Michael Z. Hu and Dr Mietek Jaroniec for useful discussions and valuable suggestions.

References

[1] E.J. Barbero, *Introduction to Composite Materials Design* (Taylor & Francis, Philadelphia, 1999).
[2] V.D. Borman, A.A. Belogorlov, A.M. Grekhov, *et al.*, JETP Lett. **74** 258 (2001).
[3] V. Eroshenko, R.C. Regis, M. Soulard, *et al.*, J. Am. chem. Soc. **123** 8129 (2001).
[4] B. Lefevre, A. Saugey, J.L. Barrat, *et al.*, J. chem. Phys. **120** 4927 (2004).
[5] Y. Qiao and X. Kong, Phys. Scripta, **71** 27–30 (2005).
[6] A.Y. Fadeev and V.A. Eroshenko, J. colloid Interface Sci. **187** 275 (1997).
[7] V.D. Borman, A.M. Grekhov and V.I. Troyan, J. exp. theor. Phys. **91** 170 (2000).

[8] T. Martin, B. Lefevre, D. Brunel, *et al.*, Chem. Commun. 24 (2002).
[9] X. Kong, F.B. Surani and Y. Qiao, J. Appl. Phys., to be published.
[10] J.A. Fay, *Introduction to Fluid Mechanics* (MIT Press, Cambridge, MA, 1997).
[11] J.M. Howe, *Interfaces in Materials* (John Wiley & Sons, New York, 1997).
[12] S.K. Milonjic, Colloids Surf. A: Physicochem. Engng Aspects **149** 461 (1999).
[13] D.D. Do and H.D. Do, Charact. Porous Solids III **87** 641 (1994).
[14] D.D. Do, H.D. Do and K.N. Tran, Langmuir **19** 5656 (2002).